Simulating Large-amplitude Membrane Motions in Inviscid Flow

University of Michigan

Christiana Mavroyiakoumou
Silas Alben

Motivation and Previous Work

A *membrane* is a thin extensible sheet with negligible bending rigidity.

- Modeling bat flights for bio-inspired robotics.
- Designing bat drones made from membrane wings for surveillance purposes.
- Interaction of membranes with flows such as air to construct efficient sails, gliders, and parachutes.
- NASA manufactured an aeroelastic micro-air vehicle with an extensible rubber membrane wing that has the ability to adapt to the airflow to provide a smoother flight compared to its rigid counterparts.

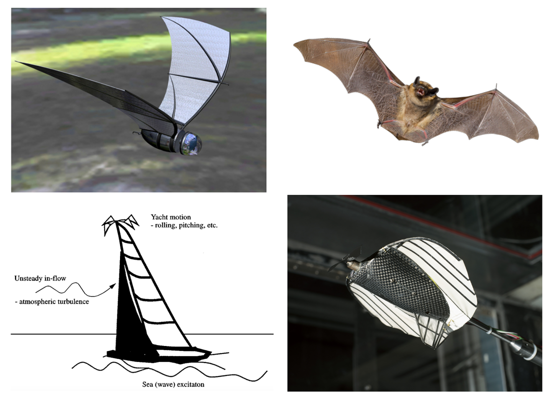

Newman & Paidoussis [NP91]
(Theoretical, 2D membrane)

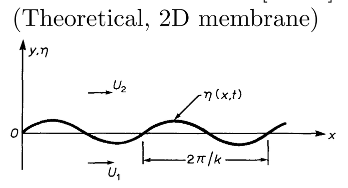

Sygulski [Syg07]
(Experimental, linear stability)

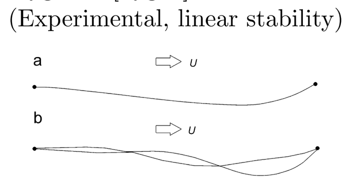

Jaworski & Gordnier [JG12] (CFD, heaving foil, thrust)

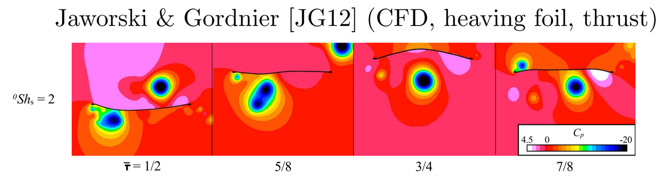

Tiomkin & Raveh [TR17]
(Stability analysis)

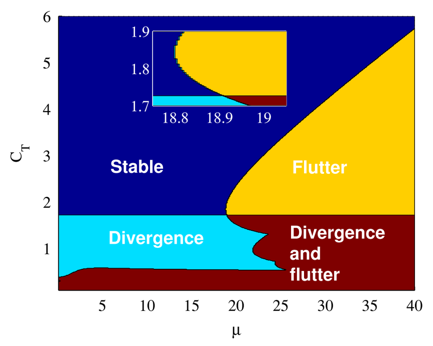

Alben & Shelley [AS08]
(Flapping flag)

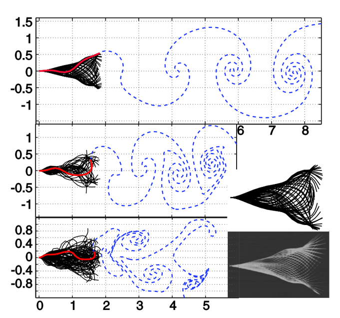

Model

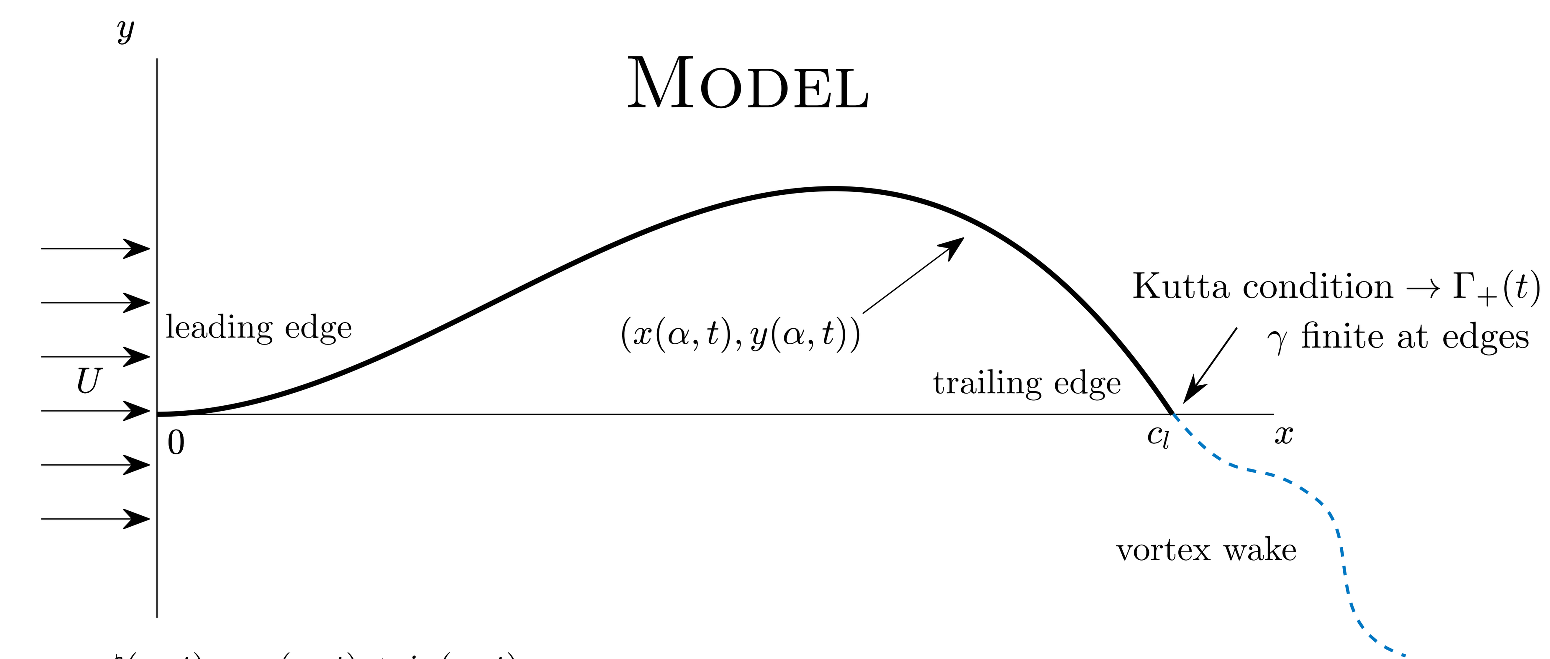

Membrane: $\zeta(\alpha,t) = x(\alpha,t) + iy(\alpha,t)$

Extensible membrane: $R_1\partial_{tt}\zeta + \underbrace{\cancel{R_2\partial_s(\partial_s\kappa(s,t)\hat{n})}}_{\text{bending resistance}} - \underbrace{\partial_\alpha((T_0 + R_3(\partial_\alpha s - 1))\hat{s})}_{\text{stretching resistance}} = -[p]\hat{n}$

Pressure jump: $\partial_\alpha s\partial_t\gamma + \gamma(\partial_\alpha\tau - \nu\kappa\partial_\alpha s) + \partial_\alpha(\gamma(\mu-\tau)) = \partial_\alpha[p]$

Birkhoff-Rott: $\partial_t\bar{\zeta}(\Gamma,t) = \dfrac{1}{2\pi i}\displaystyle\int_{-1}^{1}\frac{\gamma(\alpha',t)\partial_\alpha s(\alpha')}{\zeta(\Gamma,t)-\zeta(\alpha',t)}\,\mathrm{d}\alpha' - \frac{1}{2\pi i}\int_0^{\Gamma_+}\frac{\overline{\zeta(\Gamma,t)-\zeta(\Lambda',t)}}{|\zeta(\Gamma,t)-\zeta(\Lambda',t)|^2+\delta(\Gamma,t)^2}\,\mathrm{d}\Lambda'$

We study how the dynamics depend on three parameters:

(a) Membrane mass: $R_1 = \dfrac{\rho_s h}{0.5c_l\rho_f}$, (b) stretching rigidity: $R_3 = \dfrac{Eh}{0.5c_l\rho_f U^2}$, (c) pretension: $T_0 = \dfrac{\overline{T}}{0.5c_l\rho_f U^2 W}$.

Boundary Conditions

fixed-fixed

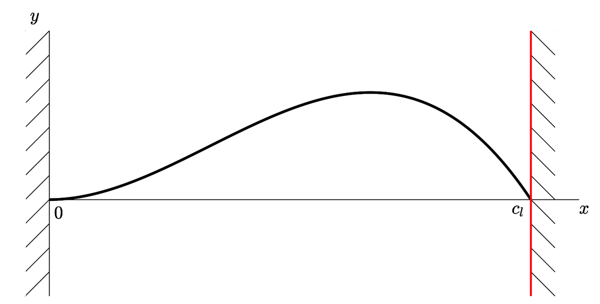

$y|_{x=0} = 0$ $\qquad y|_{x=c_l} = 0$

fixed-free

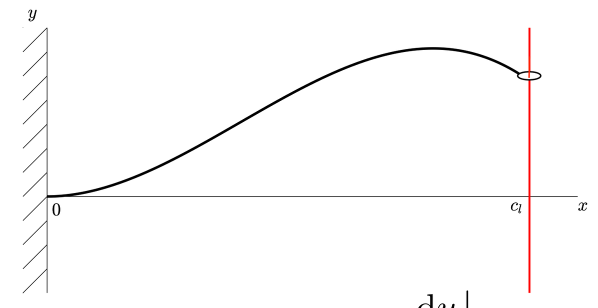

$y|_{x=0} = 0$ $\qquad \left.\dfrac{\mathrm{d}y}{\mathrm{d}x}\right|_{x=c_l} = 0$

Important Quantities

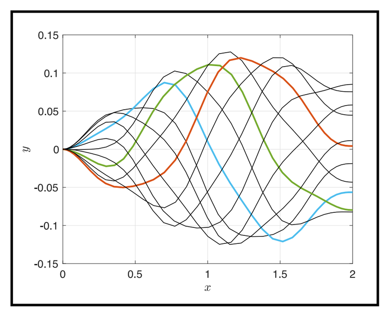

1. Zero-crossings

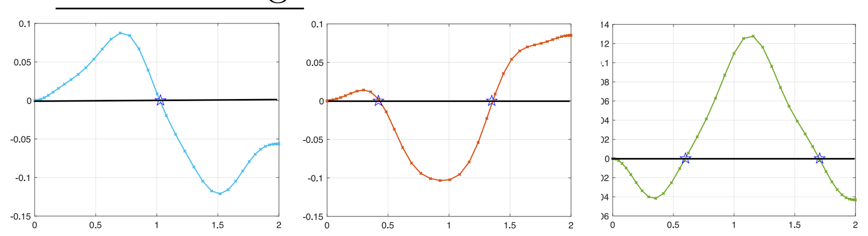

2. Amplitude

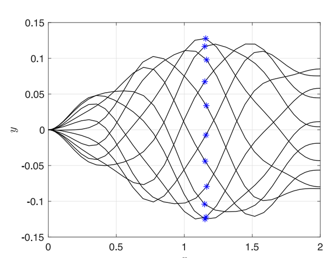

large amplitude regime

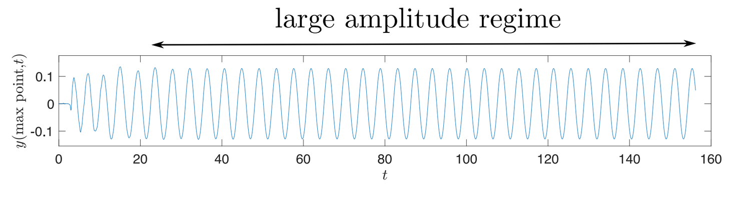

3. Frequency

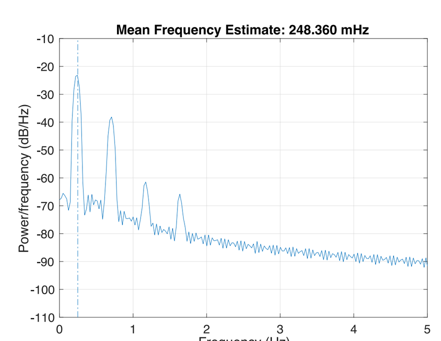

Stability Diagram (fixed-fixed)

We focus on the fixed-fixed membrane and show the stability diagram in the pretension (T_0) versus mass (R_1) parameter space. For large pretension, the membrane is stable whereas for small pretension it is unstable. The subplots show examples of the computed rates, ranging from exponential growth to exponential decay. We observe two distinct types of motion: either stable or simply divergence.

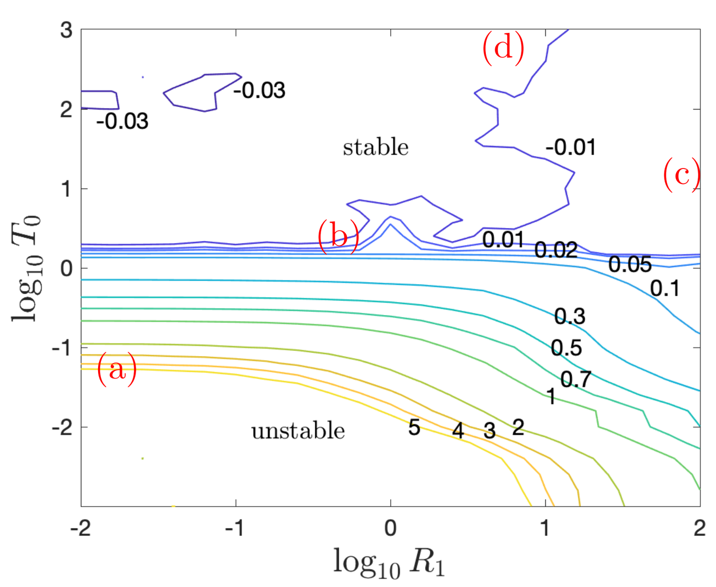

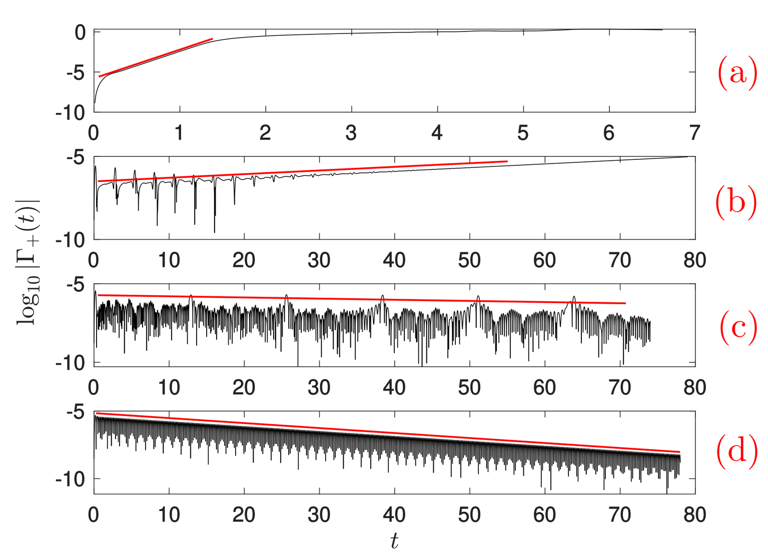

Time-averaged Amplitude

The surface plot colors correspond to the time-averaged amplitude of each membrane. We superpose mode shapes at the last time step while keeping the membrane mass fixed.

From left to right, the subplots show:

- For a specific membrane choice, how the mode shapes converge to the steady shape. In particular, we illustrate a sequence of time snapshots ranging from gray in early time to black in current time.
- All the membranes plotted on top of each other, but normalized, to emphasize that the steady shape is almost identical and it is only the amplitude that changes.
- Scaling law between time-averaged amplitude and stretching rigidity (R_3). From the governing equations, it can be shown that $y(\max) \propto 1/\sqrt{R_3}$. The different colors correspond to different pretension values T_0 but with fixed mass $R_1 = 10^{-0.5}$.

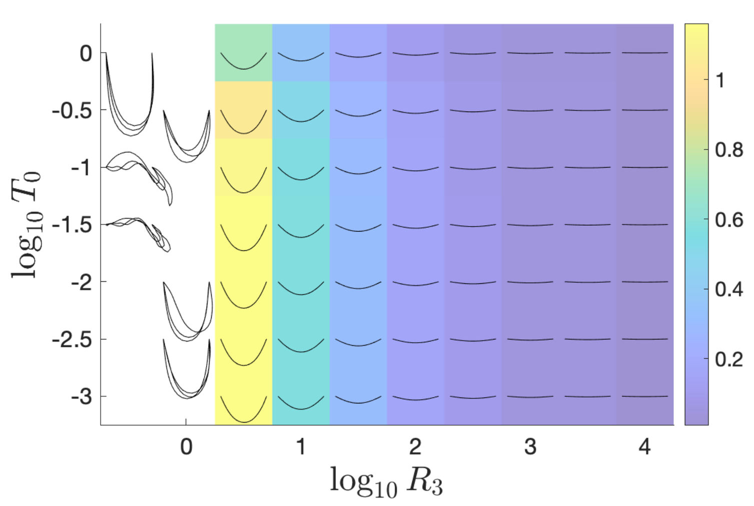

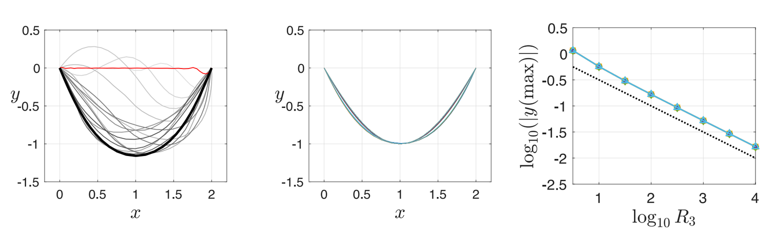

Stability Diagram (fixed-free)

Now we focus on the fixed-free membrane and show the stability diagram in the pretension (T_0) versus mass (R_1) parameter space. Similar to the fixed-fixed case, for large pretension the membrane is generally stable, and it becomes unstable for small pretension. The region of red triangles indicates where *divergence and flutter* modes exist. Membranes that exhibit this behavior have profiles such as the one shown in c).

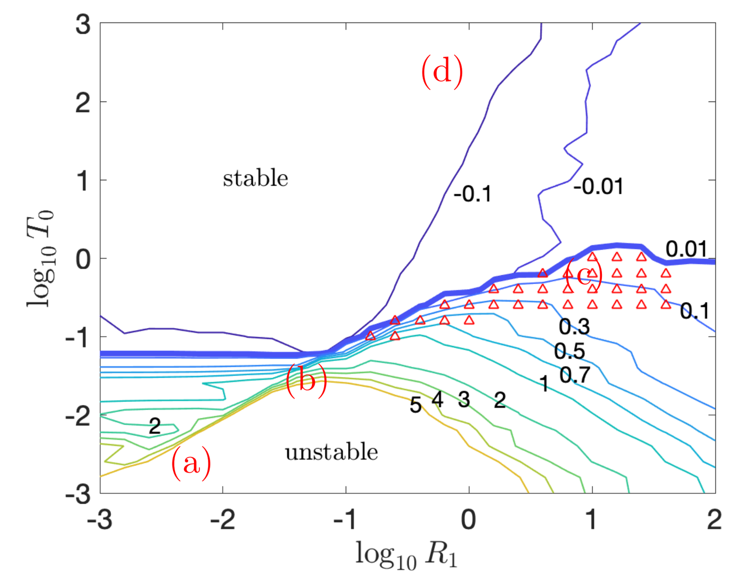

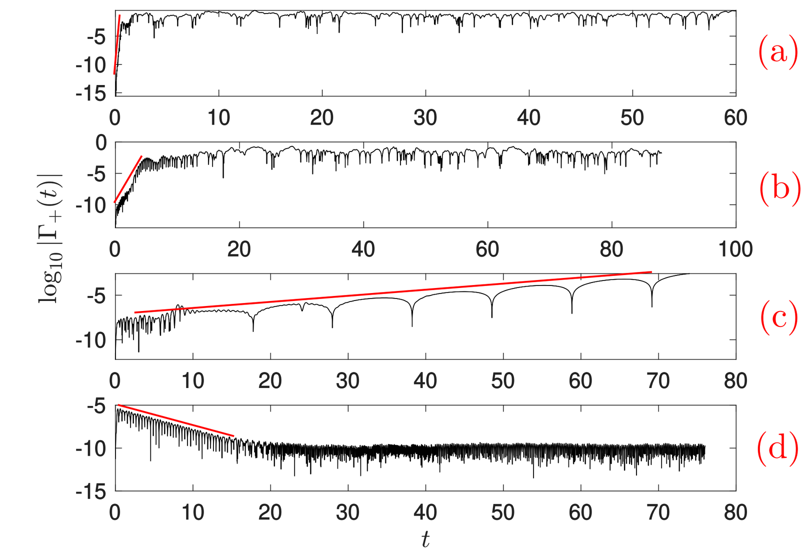

Power Spectra vs Membrane Mass and Stiffness

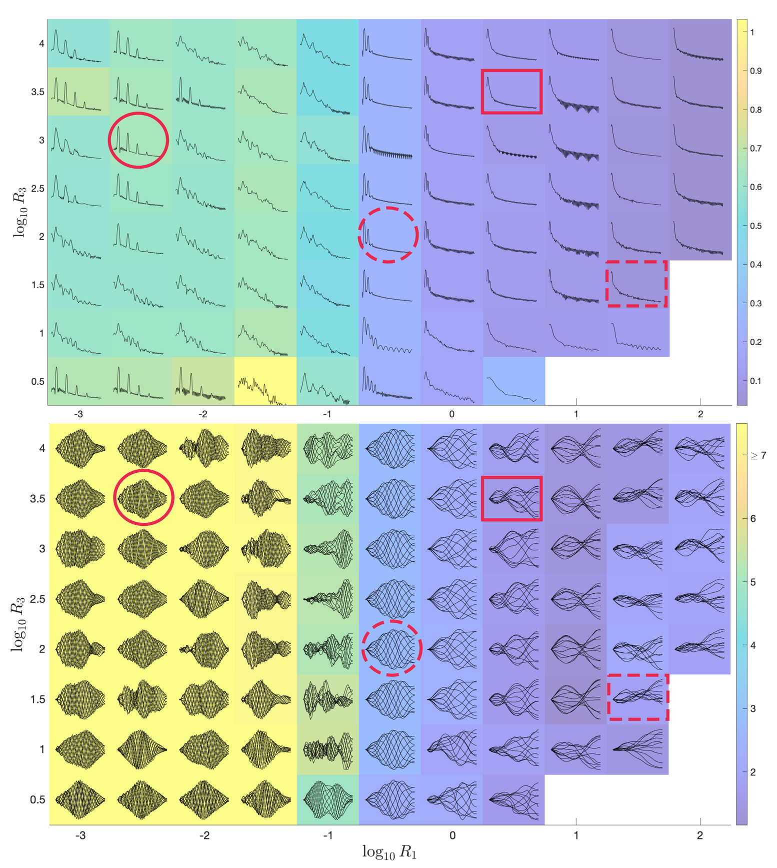

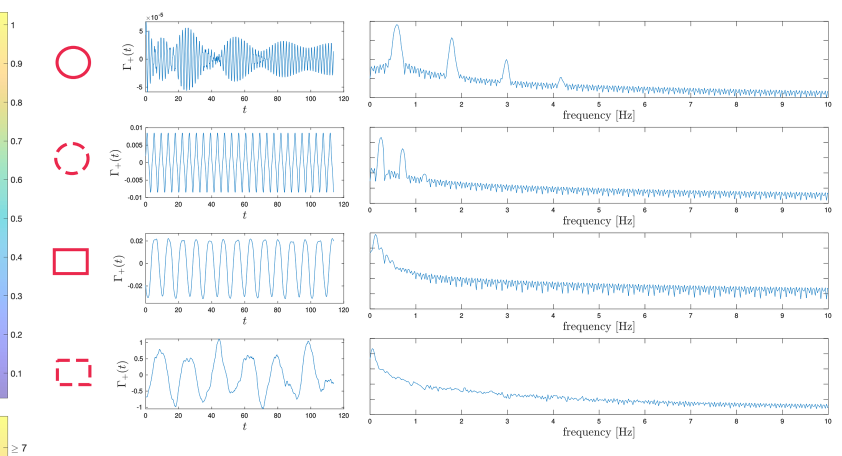

The colors of the top surface plot (left column) correspond to the mean frequency, whereas the colors of the bottom surface plot correspond to the number of zero crossings.
Wake circulation time series (middle column) and associated power spectra (right column) at different (R_1, R_3) values. We see that by increasing the mass (R_1), the system transitions to chaos. A periodic trajectory is defined by a sharply peaked spectrum at one particular frequency as well as a number of higher harmonics. A quasiperiodic trajectory is characterized by a sharply peaked spectrum at multiple irrationally related frequencies as well as a number of higher harmonics. Finally, a chaotic trajectory is characterized by a broad spectral form, or small frequency spectrum.

Scaling Laws

From the kinematic boundary condition we have

$$U\partial_\alpha y + \partial_t y \approx \hat{n}\cdot\partial_t\zeta = \mathrm{Re}\left(\frac{e^{i\theta}}{2\pi}\int_{-1}^{1}\frac{\gamma'\partial_\alpha s'}{\zeta-\zeta'}\,\mathrm{d}\alpha' + \ldots\right).$$

Recall the pressure jump equation

$$\partial_t\gamma + U\partial_\alpha\gamma \approx \partial_\alpha[p].$$

We also have $\partial_\alpha s = \sqrt{(\partial_\alpha x)^2 + (\partial_\alpha y)^2}$ and the tangential unit vector $\hat{s} = (\partial_\alpha x, \partial_\alpha y)/\sqrt{(\partial_\alpha x)^2 + (\partial_\alpha y)^2}$. Balancing terms in the extensible membrane equation

$$R_1\partial_{tt}\zeta - \partial_\alpha((T_0 + R_3(\partial_\alpha s - 1))\hat{s}) = -[p]\hat{n},$$

yields $R_3 \propto 1/\text{deflection}^2$.

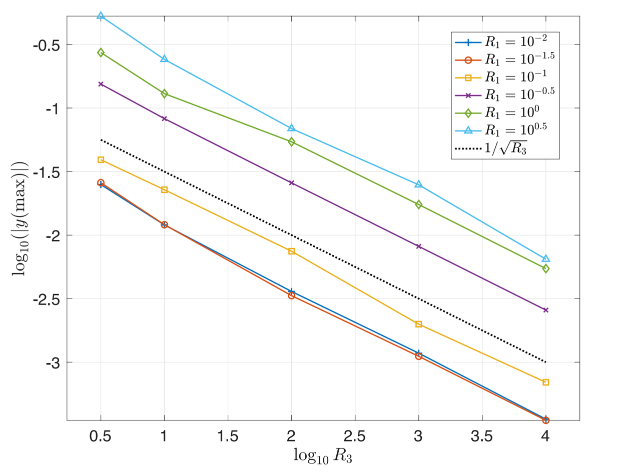

For large membrane mass values ($R_1 \geq 10$), we derive the following scaling law: $f \propto 1/\sqrt{R_1}$, where f denotes the frequency of the membrane motion.

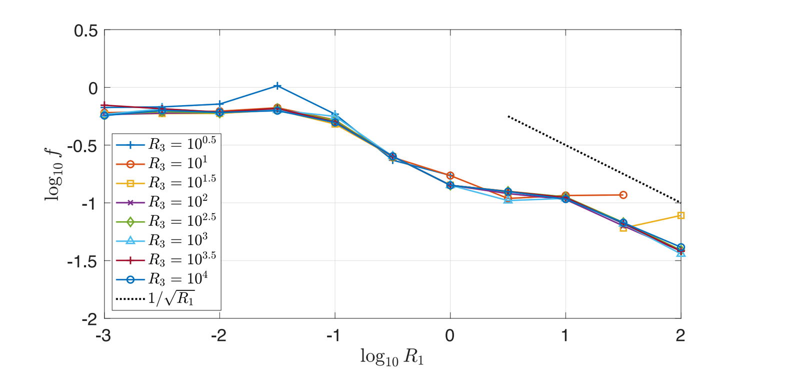

From the vortex wakes, we observe the onset of chaos for the membrane motions as the mass (R_1) increases. Furthermore, we confirm using these time snapshots, that as the stretching rigidity (R_3) increases, the amplitude of the membrane decreases.

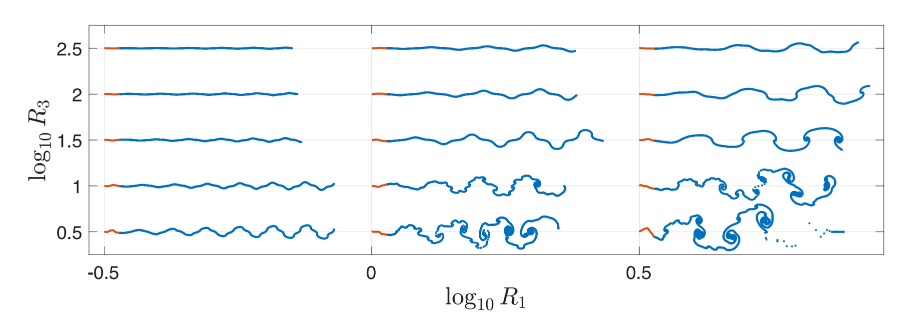

References

[Alb09] S. Alben, *Simulating the dynamics of flexible bodies and vortex sheets*, Journal of Computational Physics **228** (2009), no. 7, 2587–2603.

[AS08] S. Alben and M. J. Shelley, *Flapping states of a flag in an inviscid fluid: bistability and the transition to chaos*, Phys. Rev. Lett. **100** (2008), no. 7, 074301.

[JG12] J. W. Jaworski and R. E. Gordnier, *High-order simulations of low reynolds number membrane airfoils under prescribed motion*, J. Fluids and Struct. **31** (2012), 49–66.

[Kra86] R. Krasny, *Desingularization of periodic vortex sheet roll-up*, J. Comp. Phys. **65** (1986), no. 2, 292–313.

[NP91] B. G. Newman and M. P. Paidoussis, *The stability of two-dimensional membranes in streaming flow*, J. Fluids and Struct. **5** (1991), no. 4, 443–454.

[Syg07] R. Sygulski, *Stability of membrane in low subsonic flow*, Inter. J. of Non-Lin. Mech. **42** (2007), no. 1, 196–202.

[TR17] S. Tiomkin and D. E. Raveh, *On the stability of two-dimensional membrane wings*, J. Fluids and Struct. **71** (2017), 143–163.

Poster design adapted from A. Horawa's design.